NASA TM X-66

NOFORN

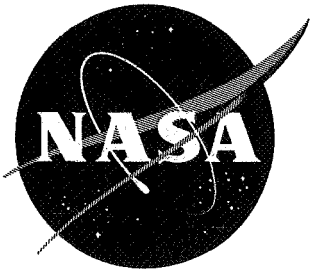

TECHNICAL MEMORANDUM

X - 66

AERODYNAMIC CHARACTERISTICS FOR TWO HYPERSONIC GLIDER MODELS WITH AND WITHOUT WING AND VERTICAL-TAIL TRAILING-EDGE CHORD-EXTENSIONS AT A MACH NUMBER OF 0.94

By F. E. West, Jr., Charles D. Trescot, Jr., and Alfred N. Wiley, Jr.

Langley Research Center
Langley Field, Va.

NATIONAL AERONAUTICS AND SPACE ADMINISTRATION
WASHINGTON
February 1960

NATIONAL AERONAUTICS AND SPACE ADMINISTRATION

TECHNICAL MEMORANDUM X-66

AERODYNAMIC CHARACTERISTICS FOR TWO HYPERSONIC GLIDER MODELS WITH AND WITHOUT WING AND VERTICAL-TAIL TRAILING-EDGE CHORD-EXTENSIONS AT A MACH NUMBER OF 0.94*

By F. E. West, Jr., Charles D. Trescot, Jr., and Alfred N. Wiley, Jr.

SUMMARY

A transonic wind-tunnel investigation has been made of two hypersonic boost-glider models with and without modifications. The basic models have highly swept clipped-tip low triangular wings and upper-surface wing-tip vertical tails that are toed in about 8°. Tests were made at angles of attack from about -1° to 19° and at an average Reynolds number, based on wing mean aerodynamic chord, of about 2.8×10^6.

The effects of adding trailing-edge chord-extensions to the wings and vertical tails were rearward shifts in center-of-pressure location, increases in static margin, and at moderate angles of attack decreases in or elimination of pitch-up tendencies. The effects of the vertical tails on normal force and pitching moment for the models with the chord-extensions were large at low angles of attack and then decreased with increasing angle at angles above 9°. Specifically, some of these effects were large negative shifts in zero-lift pitching-moment coefficient, and at moderate angles of attack increases in pitch-up tendency or at least decreases in stability. The models with the chord-extensions were directionally stable at all angles of attack and had positive effective dihedral over most of the angle range.

INTRODUCTION

An investigation has been initiated in various Langley wind-tunnel facilities to provide information from landing to hypersonic speeds on

*Title, Unclassified.

the static aerodynamic characteristics of several hypersonic boost-glider models.

This paper presents the transonic results which were obtained on two of these models with and without modifications. The basic models have highly swept clipped-tip low triangular wings and upper-surface wing-tip vertical tails that are toed in about 8°. The results show the effect on longitudinal stability of adding trailing-edge chord-extensions to the wings and vertical tails of the models. Also shown are the effects on longitudinal and lateral stability of removing the vertical tails from the configurations with the chord-extensions. The tests were made in the Langley transonic blowdown tunnel at a Mach number of about 0.94 and at angles of attack from about -1° to 19°.

SYMBOLS

The forces and moments are referenced to the body axes which have their origin on the body center line at 64 percent of the body length.

A aspect ratio

b wing span

C_N normal-force coefficient, $\frac{\text{Normal force}}{q_\infty S}$

C_Y side-force coefficient, $\frac{\text{Side force}}{q_\infty S}$

$C_{Y_\beta} = \frac{\partial C_Y}{\partial \beta}$ per degree

C_l rolling-moment coefficient, $\frac{\text{Rolling moment}}{q_\infty S b}$

$C_{l_\beta} = \frac{\partial C_l}{\partial \beta}$ per degree

C_m pitching-moment coefficient, $\frac{\text{Pitching moment}}{q_\infty S \bar{c}}$

C_n yawing-moment coefficient, $\frac{\text{Yawing moment}}{q_\infty Sb}$

$C_{n_\beta} = \frac{\partial C_n}{\partial \beta}$ per degree

$\bar{c}$ wing mean aerodynamic chord

M_∞ free-stream Mach number

q_∞ free-stream dynamic pressure

r radius

S total wing area

α angle of attack

β angle of sideslip

Model designations:

B fuselage

F wing trailing-edge chord-extension

V vertical tail

W wing

MODELS AND APPARATUS

For this investigation two basic models (designated as $B_1W_1V_1$ and $B_1W_4V_1$) and also these same two models with trailing-edge chord-extensions added were used (designated as $B_1W_1V_3F_2$ and $B_1W_4V_3F_2$). Drawings of models $B_1W_1V_3F_2$ and $B_1W_4V_3F_2$ are shown in figures 1 and 2, respectively. These models are similar to the basic models $B_1W_1V_1$ and $B_1W_4V_1$ except for the trailing-edge chord-extensions added to the wings and the vertical tails. The extensions for the vertical tails also extend below the original vertical tails. As shown in figures 1 and 2, the wing extensions are designated as F_2 and the addition of the extensions to the vertical tails changes the tail designation from V_1 to V_3.

Since the vertical tails are attached above (V_1) or above and below the wings (V_3), removal of the vertical tails (designated as configurations $B_1W_1F_2$ and $B_1W_4F_2$ without the vertical tails) does not affect the wing plan forms. The primary difference between the two basic models is that one has a straight leading edge and the other a cranked leading edge. Table I compares the wing geometry for the basic and modified configurations. The moment centers shown in this table correspond to the moment center at 64 percent of the body length. The models were mounted on an internal 5-component electrical strain-gage balance that was attached to the sting-support system in the Langley transonic blowdown tunnel. This tunnel has an octagonal slotted throat section measuring 26 inches between flats.

TESTS

Normal-force, pitching-moment, rolling-moment, yawing-moment, and side-force data were obtained for all configurations. The tests were made at a tunnel stagnation pressure of 25 pounds per square inch absolute, a Mach number of about 0.94, and angles of attack which varied from about -1° to a maximum of 19°. All configurations were tested at an angle of sideslip of 0°, and configurations $B_1W_1V_3F_2$, $B_1W_1F_2$, $B_1W_4V_3F_2$, and $B_1W_4F_2$ were also tested at a nominal angle of sideslip of 5°.

Transition strips consisting of 0.001- to 0.002-inch carborundum grains spread on a thin wet coating of shellac were applied to the model surfaces. (See ref. 1.) They were about 1/16 inch wide and the grains covered 5 to 10 percent of the strip areas. These strips were put on the upper and lower surfaces of the wing, the side surfaces of the tails, and around the periphery of the body nose. Leading edges of the strips were located at 5 percent of the wing chord, 7.5 percent of the vertical-tail chord, and at the line of tangency of the body nose and nose cone. Average Reynolds number based on the model mean aerodynamic chords was about 2.8×10^6.

PRECISION

Estimated accuracy of coefficients (based on balance accuracy), and other pertinent parameters are indicated below:

C_N	± 0.01
C_m	± 0.002
C_l	± 0.001

C_n	±0.002
C_Y	±0.004
α, deg	±0.1
β, deg	±0.1
M_∞	±0.02

No corrections due to tunnel-wall effects or sting interference have been applied to the data. It is believed that these corrections would be small. (See refs. 2 and 3.)

RESULTS AND DISCUSSION

The effects on the normal-force and pitching-moment characteristics of adding the trailing-edge chord-extensions to the two basic models are shown in figures 3 and 4, respectively. The effects on these same characteristics of removing the vertical tails from the models with the extensions are shown in figures 5 and 6, respectively. Summary curves showing the variation of longitudinal center-of-pressure location and longitudinal stability parameter with normal-force coefficient for the various configurations are presented in figures 7 and 8. Figure 9 shows the effects on lateral stability derivatives of removing the vertical tails from the models with the extensions.

If desired, the normal-force results presented in this paper can probably be used to estimate lift coefficient with good accuracy, since unpublished Langley 16-foot transonic tunnel data on a configuration somewhat similar to model $B_1W_1V_1$ indicates excellent agreement between lift coefficient and $C_N \cos \alpha$ for the angle-of-attack range investigated in the present tests.

Normal-Force Characteristics

Perhaps the normal-force characteristics of most interest are those which show the effect of the vertical tails. (See fig. 5.) Without the tails on the models, the normal-force curves were nonlinear. At low angles of attack the experimental slopes corresponded approximately to linear theory predictions. At moderate angles the experimental slopes increased. These increases are typical for low-aspect-ratio wings at both subsonic and transonic speeds (for example, see ref. 4) and are associated with viscous effects on the wing upper surfaces. Reference 5 presents a method for predicting the nonlinear effects which is based on linear lifting-surface theory plus viscous cross-flow theory. That is, an α^2 term is added to the linear-theory term and the constant of

proportionality for this squared term is dependent upon the shape of the side edges of the wing. For a wing with square edges the constant would be 2, since that is the drag coefficient of a flat plate of zero aspect ratio placed perpendicular to the stream. After a study of reference 5 a value of 1.5 was estimated for the constant in the case of the present models, as shown by the following equation:

$$C_N = \alpha \frac{\partial C_N}{\partial \alpha} + 1.5\alpha^2$$

Results obtained from this equation, in which the first term is based on the theory presented in reference 6, are shown in figure 5. These results, which do not include the effects of the negative camber or body, show fair agreement in slope with the experimental normal-force curve slopes.

L 6 3 0

Figure 5 shows that adding the tails to the models increased the normal-force coefficients and the normal-force curve slopes at the low angles and caused the curves to become linear over most of the angle range. The increases in slope and changes in linearity of the normal-force curves are associated with the end-plate effects of the vertical tails; that is, the tails increased the effective aspect ratios of the models. The increases in normal-force coefficient at low angles of attack resulted from the toe-in (about 8°) effect of the vertical tails creating low-pressure regions over the outboard sections of the wing upper surfaces. At higher angles, the normal-force curves for the tail-on and tail-off configurations tend to approach each other. This effect is probably associated with a leading-edge separation vortex-type flow and shocks (for example, see ref. 7) that had an increasingly predominant influence on the outboard upper-surface flow as the angle of attack was increased. That is, the outboard flow separation caused by the vortex flow and shocks at the higher angles reduced the effect of the vertical tails on the wing pressures.

Pitching-Moment Characteristics

The curves of figures 4 and 7 show, as would be expected, that the addition of wing area behind the wing trailing edges caused rearward shifts in center-of-pressure location $\left(C_m/C_N\right)$ and increases in static margin $\left(\partial C_m/\partial C_N\right)$. The decreases or elimination of the pitch-up tendencies at moderate angles of attack caused by the addition of the chord-extensions appear to be due mostly to the increased static margin rather than to any improvement of the flow over the wings.

Figures 6 and 8 show that two of the effects of the vertical tails were to increase the absolute magnitude of the zero-lift pitching-moment

coefficients, and at moderate angles of attack to increase the pitch-up tendencies or at least to decrease the stability. Other effects were rearward movements in the center-of-pressure locations, increased static margins at low normal-force coefficients, and decreased margins at the high normal-force coefficients. These changes are all associated with the effects of the tails on the pressures over the outboard sections of the wing upper surfaces. As indicated in the discussion of normal-force characteristics, the tail effects on the pressures were large in the lower angle range and then decreased with increasing angle above an angle of attack of about 9°.

Lateral Stability Characteristics

The results of figure 9 based on tests at angles of sideslip of about 0° and 5° show that the models with the tail on were directionally stable at all angles investigated and had positive effective dihedral over most of the angle range. Removal of the vertical tails from the models caused directional instability at all angles and slight decreases in effective dihedral at low angles.

CONCLUSIONS

A wind-tunnel investigation has been made of two hypersonic boost-glider models with and without modifications. The basic models have highly swept clipped-tip low triangular wings and upper-surface wing-tip vertical tails that are toed in about 8°. Results of the investigation which were obtained at a Mach number of about 0.94 and at angles of attack from about -1° to 19° indicate the following:

1. The effects of adding trailing-edge chord-extensions to the wings and vertical tails were rearward shifts in center-of-pressure location, increases in static margin, and at moderate angles of attack decreases or elimination of the pitch-up tendencies.

2. The effects of the vertical tails on normal force and pitching moment for the models with the chord-extensions were large at low angles of attack and then decreased with increasing angle at angles above about 9°. At low angles some of these effects were increases in the normal-force curve slopes and the normal-force coefficients and large negative shifts in pitching-moment coefficient. At moderate angles their effect was to increase the pitch-up tendencies or at least to decrease stability.

3. The models with the trailing-edge chord-extensions and tails on were directionally stable at all angles of attack and had positive effective dihedral over most of the angle range. Removal of the tails

from the models caused directional instability at all angles and slight decreases in effective dihedral at low angles.

Langley Research Center,
National Aeronautics and Space Administration,
Langley Field, Va., June 25, 1959.

REFERENCES

1. Braslow, Albert L., and Knox, Eugene C.: Simplified Method for Determination of Critical Height of Distributed Roughness Particles for Boundary-Layer Transition at Mach Numbers From 0 to 5. NACA TN 4363, 1958.

2. Whitcomb, Charles F., and Osborne, Robert S.: An Experimental Investigation of Boundary Interference on Force and Moment Characteristics of Lifting Models in the Langley 16- and 8-Foot Transonic Tunnels. NACA RM L52L29, 1953.

3. Cahn, Maurice S.: An Experimental Investigation of Sting-Support Effects on Drag and a Comparison With Jet Effects at Transonic Speeds. NACA Rep. 1353, 1958. (Supersedes NACA RM L56F18a.)

4. Hall, Charles F.: Lift, Drag, and Pitching Moment of Low-Aspect-Ratio Wings at Subsonic and Supersonic Speeds. NACA RM A53A30, 1953.

5. Flax, A. H., and Lawrence, H. R.: The Aerodynamics of Low-Aspect-Ratio Wings and Wing-Body Combinations. Rep. No. CAL-37, Cornell Aero. Lab., Inc., Sept. 1951.

6. Lomax, Harvard, and Sluder, Loma: Chordwise and Compressibility Corrections to Slender-Wing Theory. NACA Rep. 1105, 1952. (Supersedes NACA TN 2295.)

7. West, F. E., Jr., and Henderson, James H.: Relationship of Flow Over a 45° Sweptback Wing With and Without Leading-Edge Chord-Extensions to Longitudinal Stability Characteristics at Mach Numbers From 0.60 to 1.03. NACA RM L53H18b, 1953.

TABLE I

ADDITIONAL MODEL PHYSICAL CHARACTERISTICS

Model	A	b, in.	$\bar{c}$, in.	S, sq in.	Moment center, percent $\bar{c}$
$B_1W_1V_1$	0.98	3.28	4.24	11.01	49
$B_1W_1V_3F_2$	1.00	3.46	4.27	12.02	37
$B_1W_4V_1$	1.19	3.62	4.000	11.04	46
$B_1W_4V_3F_2$	1.18	3.80	4.02	12.21	33

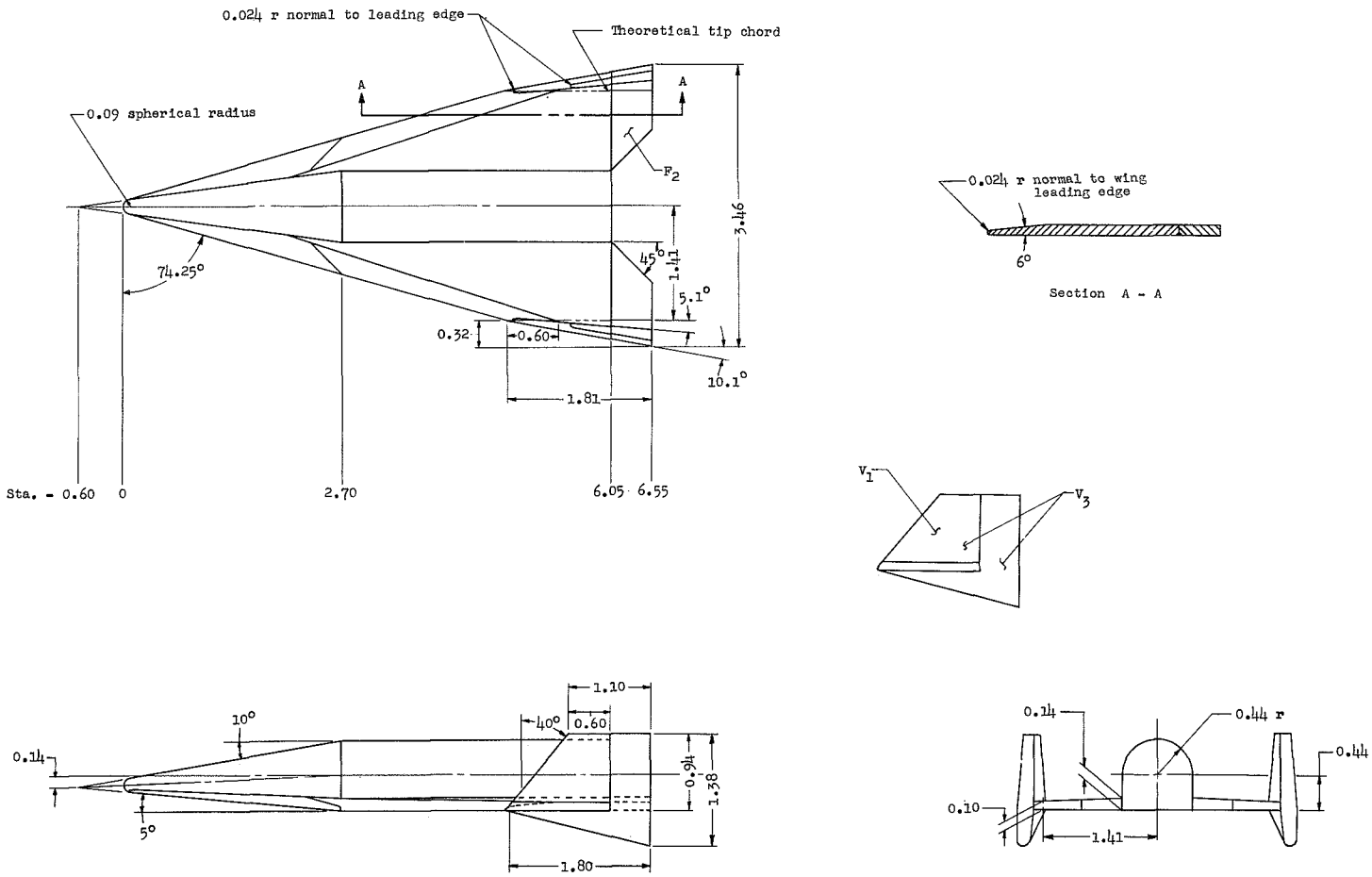

Figure 1.- Drawings of model $B_1W_1V_3F_2$. All dimensions are in inches unless otherwise indicated.

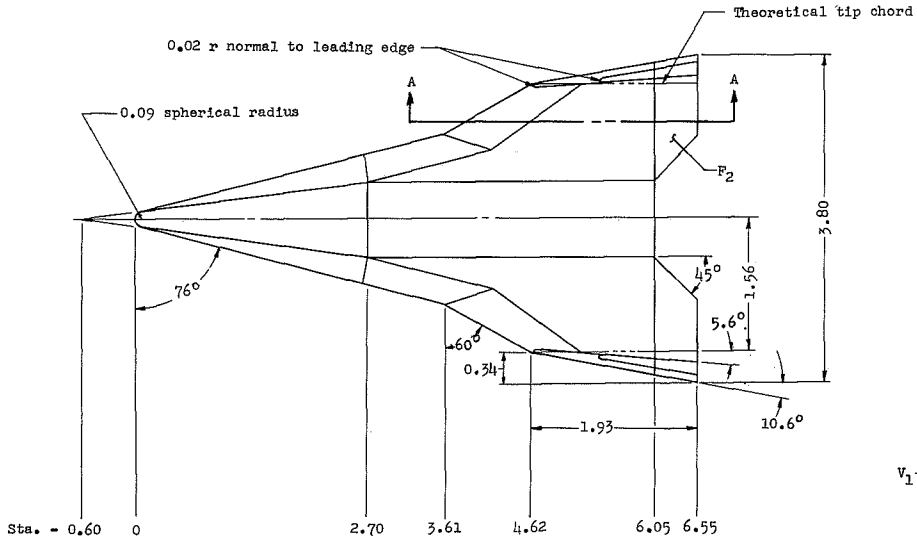

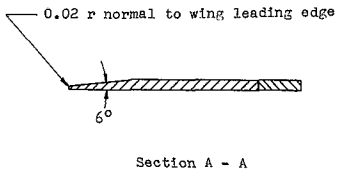

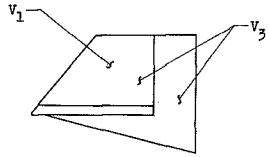

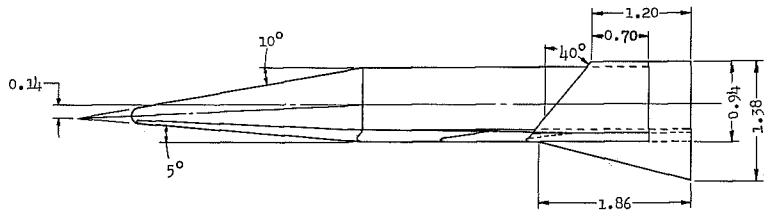

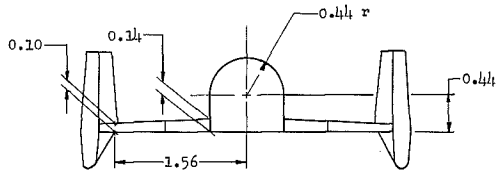

Figure 2.- Drawings of model $B_1W_4V_3F_2$. All dimensions are in inches unless otherwise indicated.

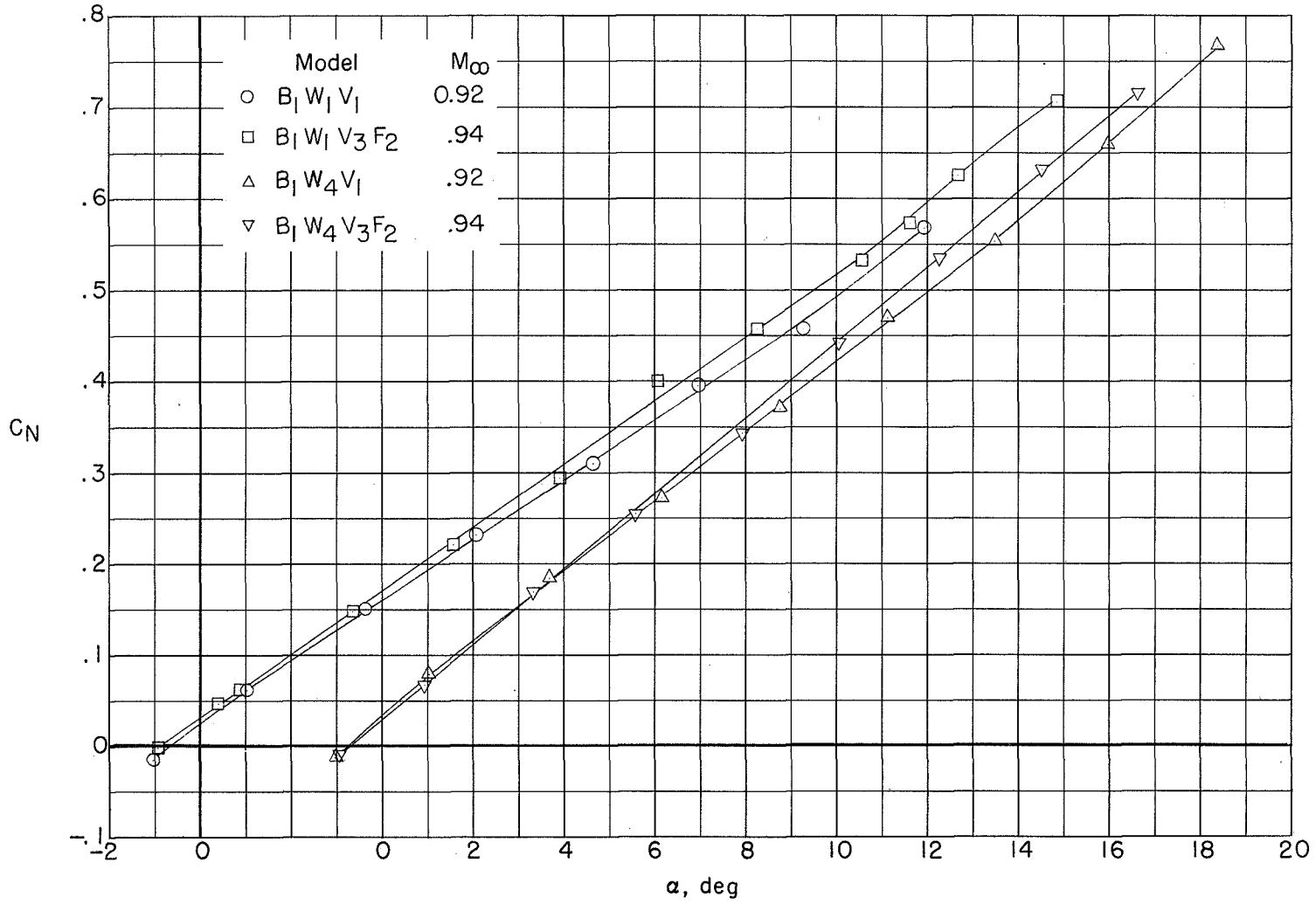

Figure 3.- Effect of trailing-edge extensions on the variation of normal-force coefficient with angle of attack.

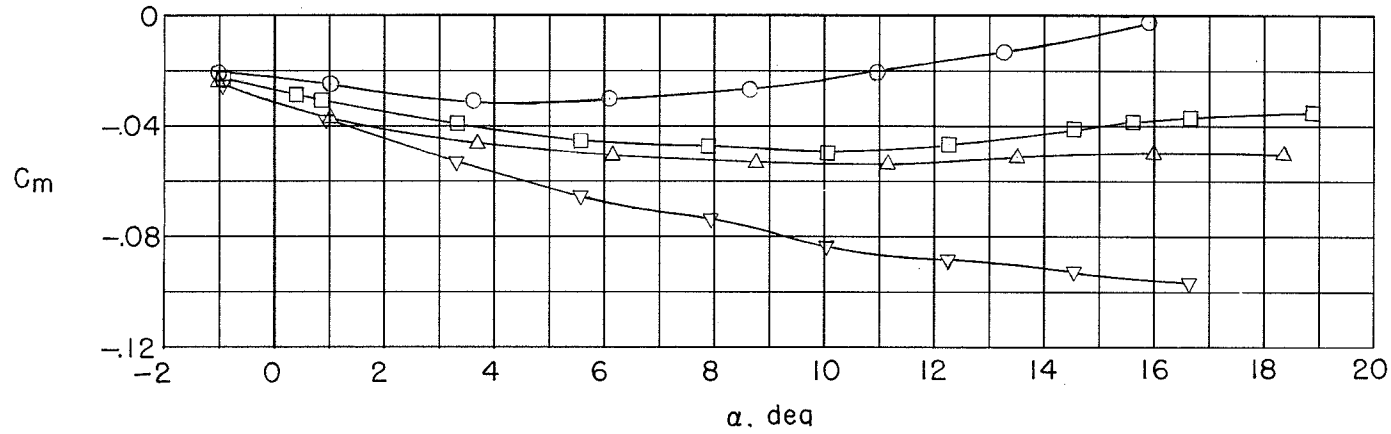

(a) C_m against α.

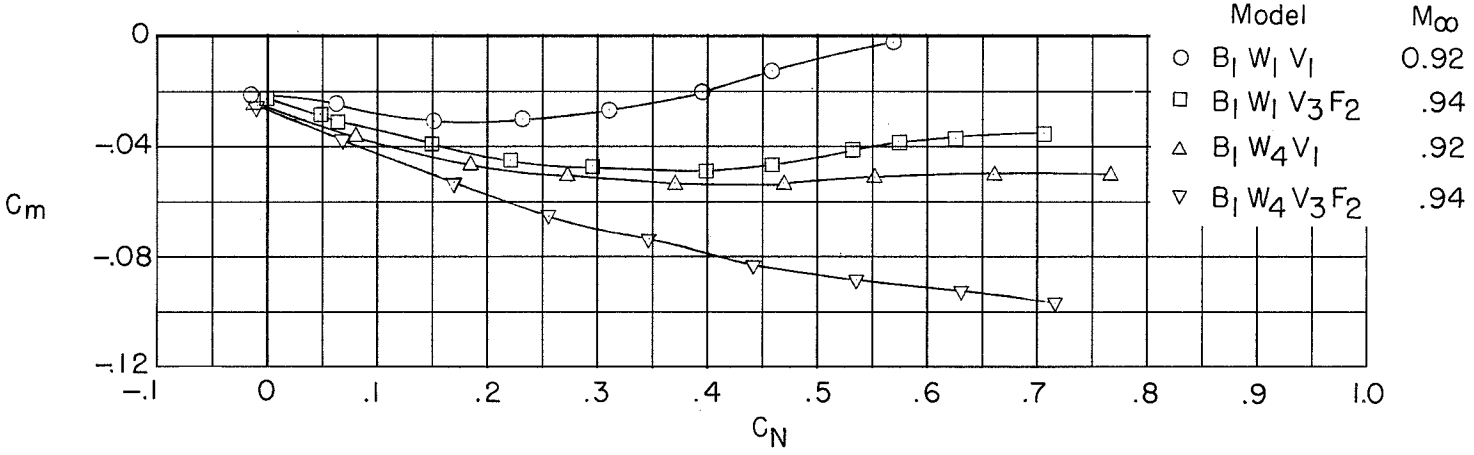

(b) C_m against C_N.

Figure 4.- Effect of trailing-edge extensions on the variation of pitching-moment coefficient with angle of attack and normal-force coefficient.

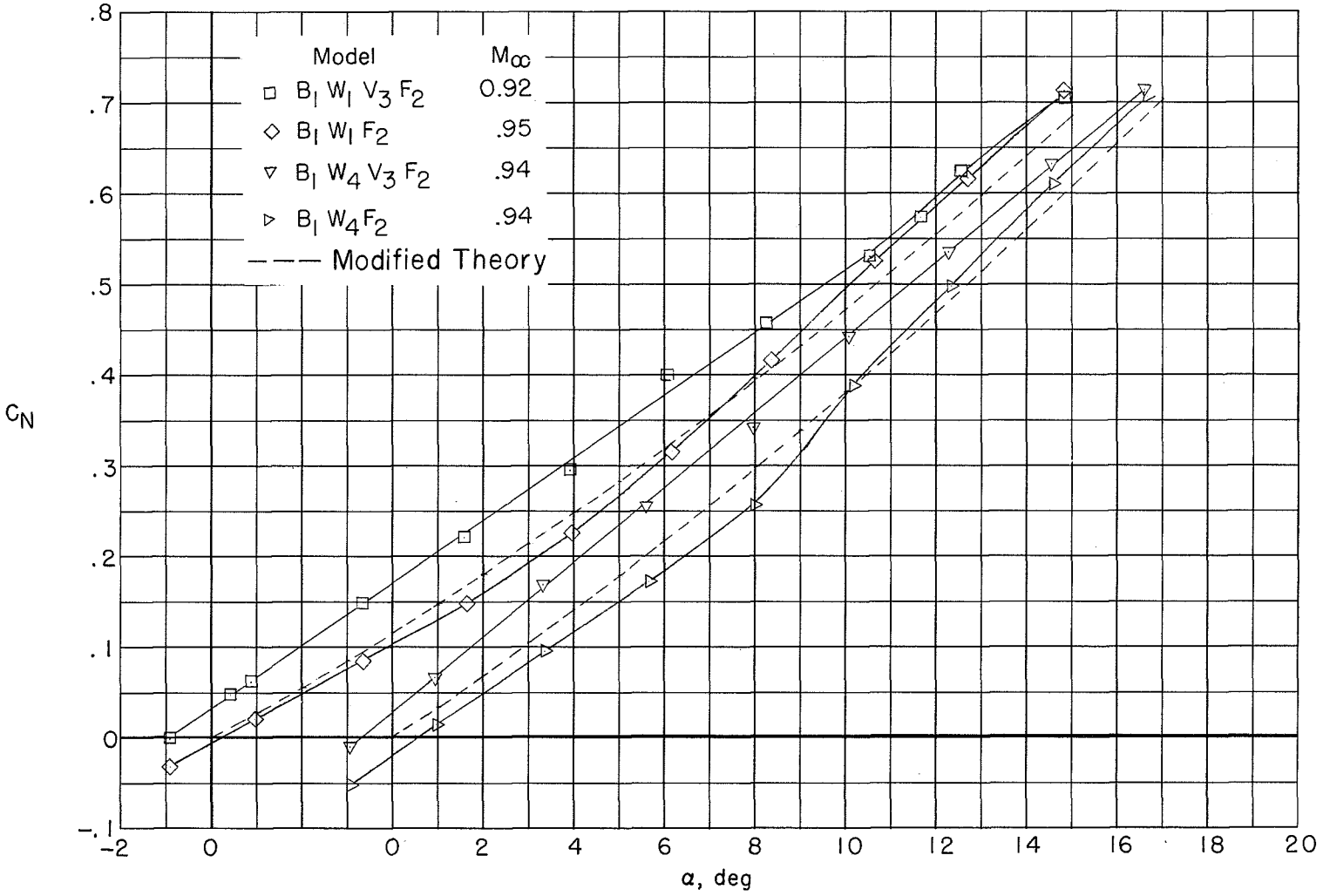

Figure 5.- Effect of vertical tails on the variation of normal-force coefficient with angle of attack for models with trailing-edge extensions.

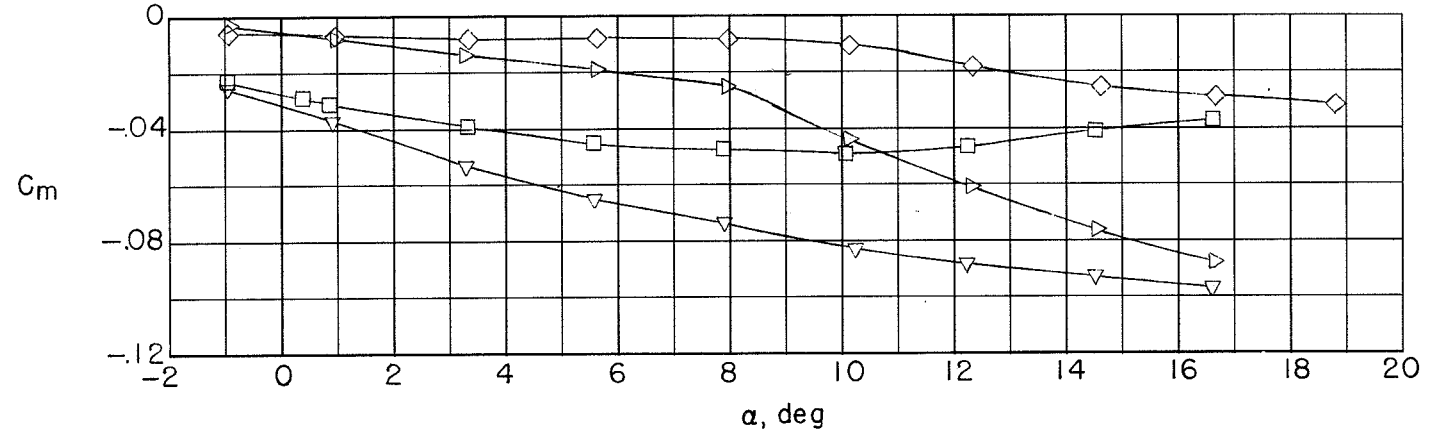

(a) C_m against α.

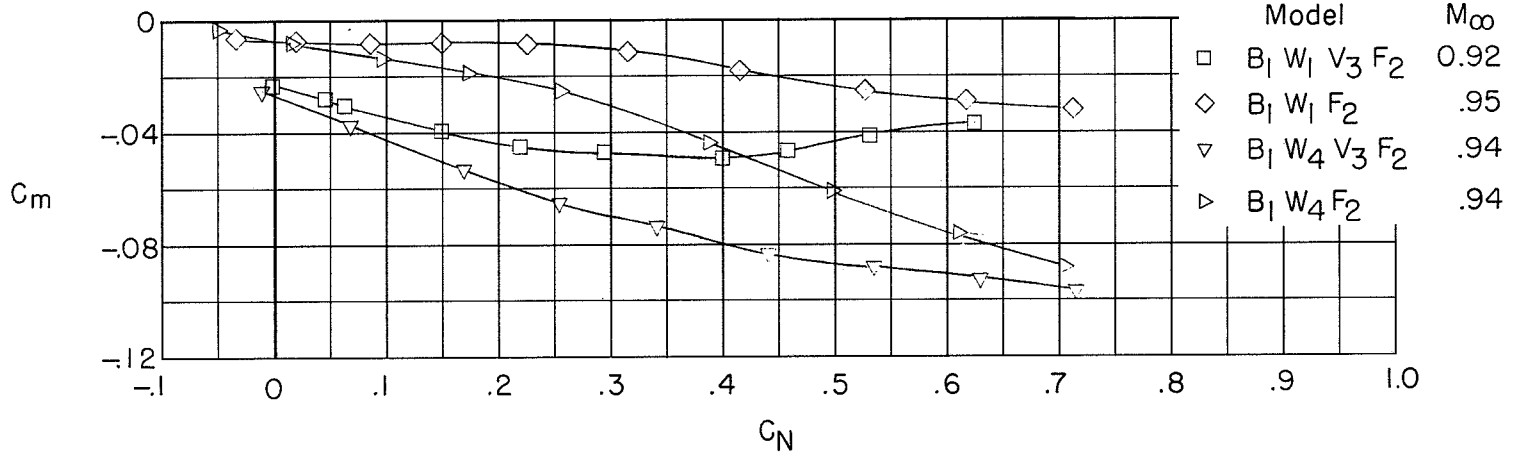

(b) C_m against C_N.

Figure 6.- Effect of vertical tails on the variation of pitching-moment coefficient with angle of attack and normal-force coefficient for models with trailing-edge extensions.

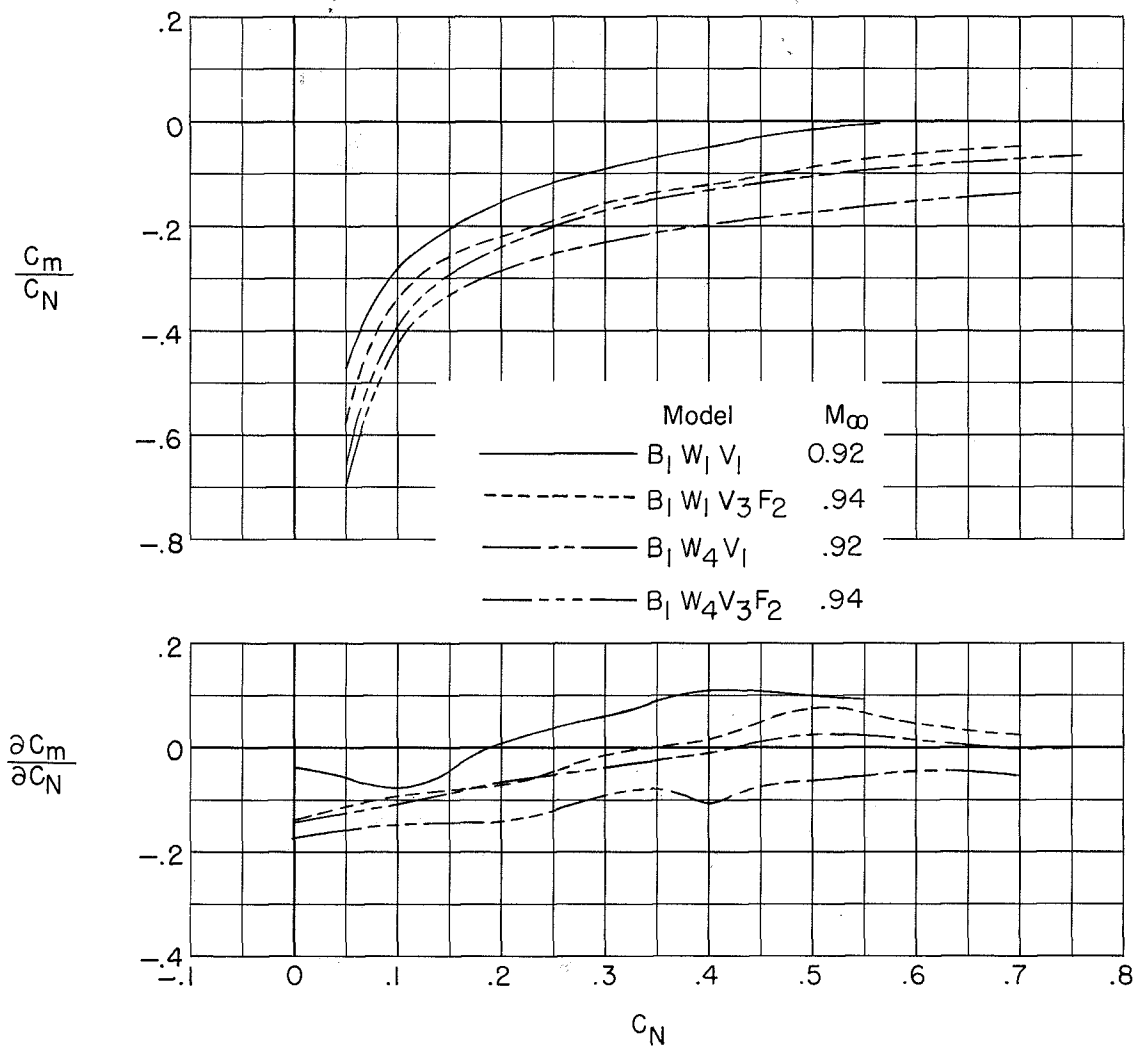

Figure 7.- Effect of trailing-edge extensions on the variation of longitudinal center-of-pressure location and longitudinal stability parameter with normal-force coefficient.

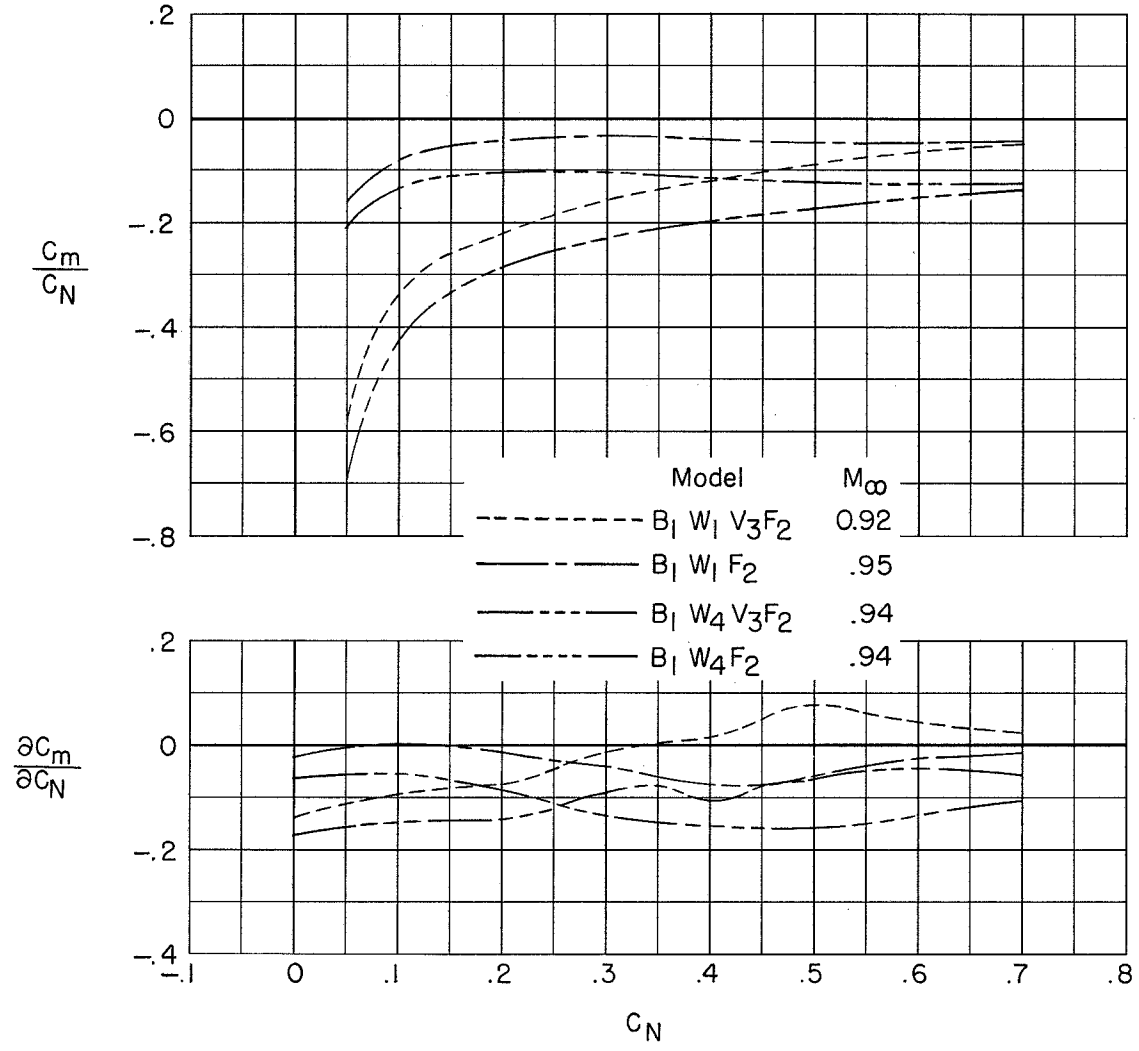

Figure 8.- Effect of vertical tails on the variation of longitudinal center-of-pressure location and longitudinal stability parameter with normal-force coefficient.

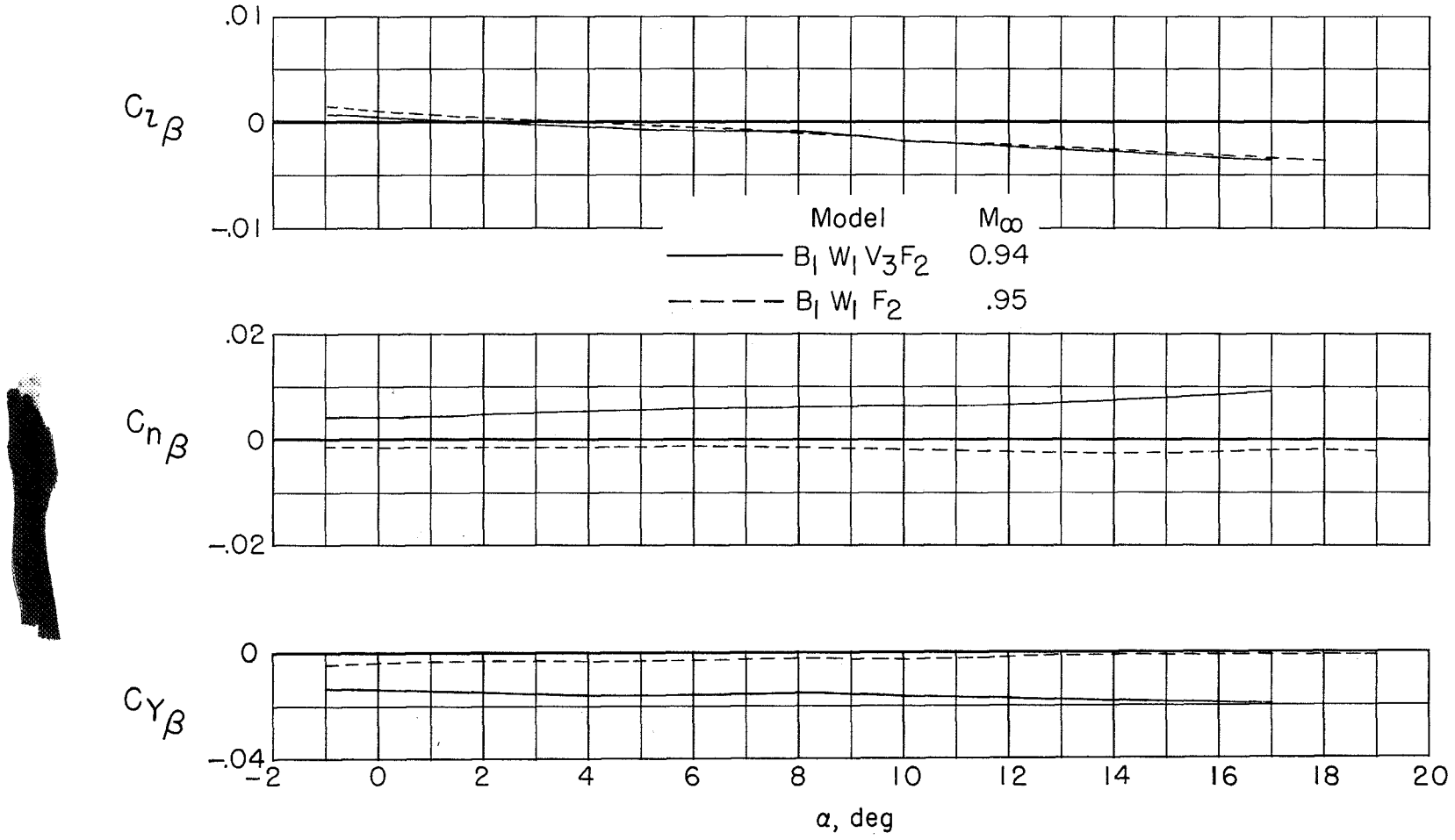

(a) $B_1W_1V_3F_2$ and $B_1W_1F_2$.

Figure 9.- Variation of lateral stability derivatives with angle of attack for models with trailing-edge extensions.

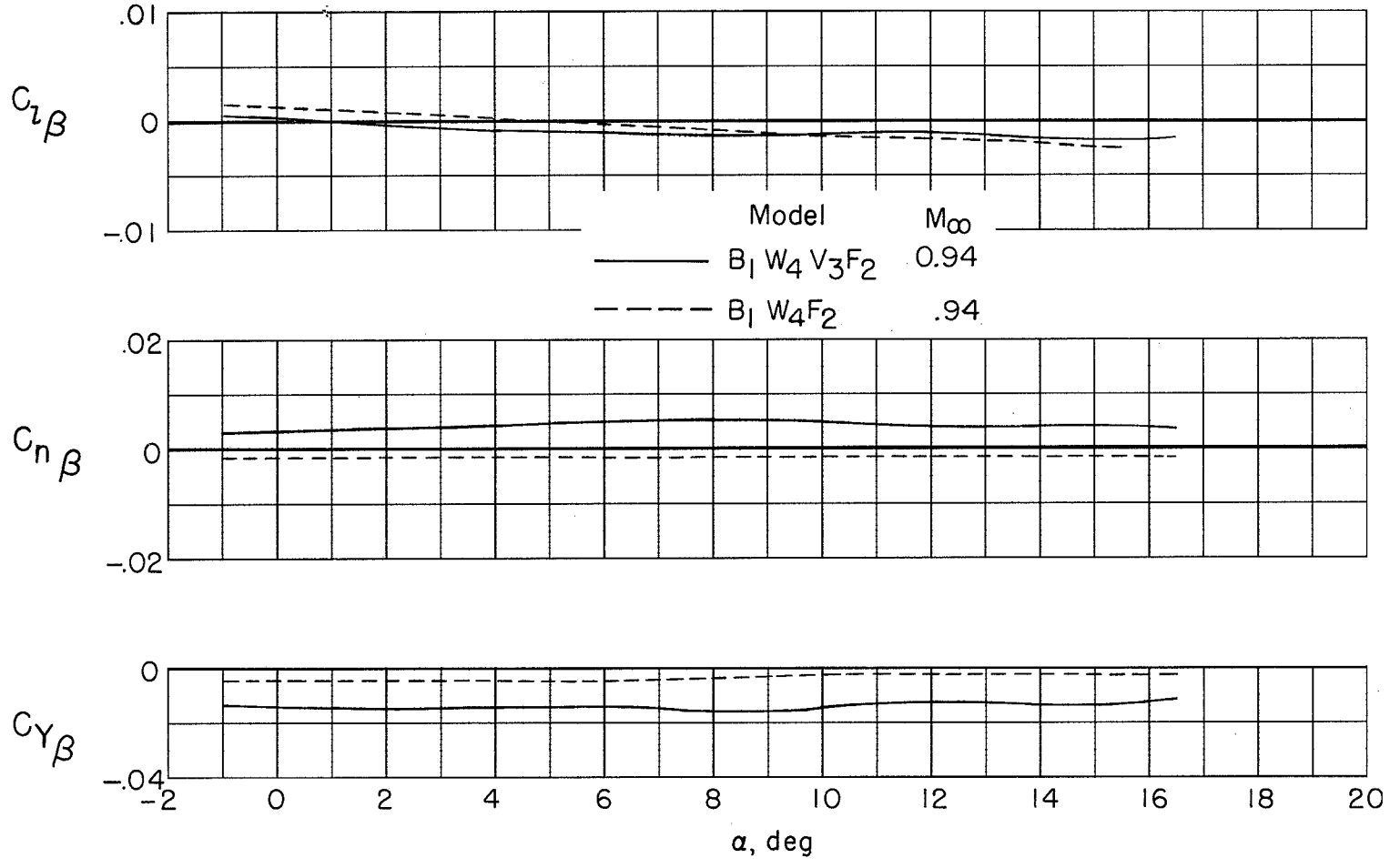

(b) $B_1W_4V_3F_2$ and $B_1W_4F_2$.

Figure 9.- Concluded.